

MINIATURIZATION DESIGN OF FULL DIFFERENTIAL BANDPASS FILTER WITH COUPLED RESONATORS USING EMBEDDED PASSIVE DEVICE TECHNOLOGY

S.-M. Wu^{*}, C.-T. Kuo, P.-Y. Lyu, Y.-L. Shen, and C.-I. Chien

Department of Electrical Engineering, National University of Kaohsiung, No. 700, Kaohsiung University Road, Nan-Tzu District, Kaohsiung 811, Taiwan

Abstract—This paper presents two full differential bandpass filters with small occupied areas. Both filters are designed with the same basic structure which consists of two double coupled resonators with magnetic coupling. The resonators are stacked up and have the advantage of high coupling efficiency, reducing the area. Nevertheless, in the basic structure, the insertion loss in the high stopband is above -10 dB and therefore does not meet the requirement for bandpass filter design. Thus, two solutions are introduced to form the proposed filters. The first one integrates the ground plane, while the second one makes the use of an extra transmission zero. With the help of these solutions, two types of full differential bandpass filters are implemented on an FR4 using the embedded passive device technology, with the additional purpose of being designed for SiP applications. The passband of the filters conforms to the WLAN IEEE 802.11a (5 GHz) standard. Most importantly, the occupied areas of the two proposed bandpass filters are only $6\text{ mm} \times 6.7\text{ mm}$ and $6.6\text{ mm} \times 8.3\text{ mm}$ respectively. Compared with previous research, area reductions of up to 98.05% and 97.76% can be achieved.

1. INTRODUCTION

The superheterodyne receiver is a common component in communication systems. Due to its high selectivity and high sensitivity, it is widely used in radios, televisions, radars and mobile phones. A traditional superheterodyne receiver mainly contains a low noise amplifier (LNA), a mixer, an analog-to-digital converter (ADC), and some bandpass

Received 14 September 2011, Accepted 19 October 2011, Scheduled 1 November 2011

^{*} Corresponding author: Sung-Mao Wu (sungmao@nuk.edu.tw).

filters [1]. More and more receivers are being designed to use a differential signal rather than a single-end signal, for the following reasons. First, a differential signal has higher noise immunity than a single-end signal [2]. A differential signal is based on a set of signals equal in magnitude but opposite in phase. There is a virtual ground between the two signal paths due to signal subtraction. A differential signal takes an ideal ground for reference while a single-end signal takes the normal ground plane for reference. Second, an amplifier designed for a differential signal will have a high differential-mode gain, high input impedance and low output impedance [3]. Third, a double-balanced active mixer, also known as a Gilbert mixer [4], has the advantages of good isolation and even harmonic suppression of the signal. Last, the amplitude of a differential signal is twice as that of a single-end signal, which would aid in system translation from analog to digital in the ADC. For coordinated operation, other devices such as bandpass filters tend to be designed for a differential signal.

The bandpass filter is a device for eliminating unnecessary signals, which regarded as noise. Filters are essential for most of the communication products. Many structures have been proposed in previous researches. A step impedance resonator was used in [5–8]. The filter in [9] employed quarter-wavelength ($\lambda/4$) resonators, and [10,11] employed half-wavelength ($\lambda/2$) resonators. The filter in [12,13] were designed with a parallel strip line (PSL) and double-sided parallel strip line (DSPSL), respectively. Study [14] simply used a microstrip line while [15–17] also used branch-line and open-circuited stubs. However, these studies were all designed on a transmission line, and the transmission line characteristics limited the possibilities for area reduction, necessitating the introduction of an embedded passive component.

For most of electronic communication products, the number of passive component and their occupied areas are both greater than those of the active components. Following the trend of product miniaturization, many kinds of technology have been introduced to improve processes and materials. At the same time, integrated passive components have been developed to replace surface mounted devices (SMDs). In recent years, low temperature co-fired ceramic (LTCC) technology has become popular [18,19], but its high cost is a drawback. For this reason, embedded passive device technology is being explored. Embedded passive devices contain circuits in a multi-layer structure or directly on the package substrate. Compared to SMDs, embedded passive devices can increase the number of components in the same area with the help of circuit integration. Furthermore, reducing the weld can increase reliability and reduce parasitic effects at high frequencies.

Embedded passive device technology is commonly used to design passive circuits in system in package (SiP) technology, which puts many chips and passive components in a package [20]. In comparison, system on chip (SoC) technology includes many circuits on a chip. SoC could be consisted in SiP, and SiP is a simplification of SoC. The most remarkable advantage of SiP is that all of the circuits can be easily developed individually, saving money and time [21]. In addition, the passive components designed in the CMOS process decrease quality factor and increase loss. Thus, the passive components in SiP perform better than SoC.

In this paper, two full differential bandpass filters are implemented on FR4 for WLAN IEEE 802.11a (5 GHz) applications. Figure 1 illustrates a cross-section of the substrate. In the process of designing this bandpass filter, a full wave simulation Ansoft HFSSTM is used. The proposed bandpass filters are both designed on the same basic structure, which consists of two resonators with magnetic coupling that form the transformer base. The symmetrical structure is conducive to common-mode suppression. To reduce the occupied area, the coils in the resonators are stacked, yielding high coupling efficiency. The equivalent circuit of the proposed structure is the same as the design in [22], which employed an interactive wound coil. Mutual inductance is formed by lateral coupling, but the transmission zero in the low stopband does not appear. However, the proposed structure in this paper can provide two transmission zeros near the passband, and it enhances the filter performance.

However, in the basic structure, the differential-mode insertion

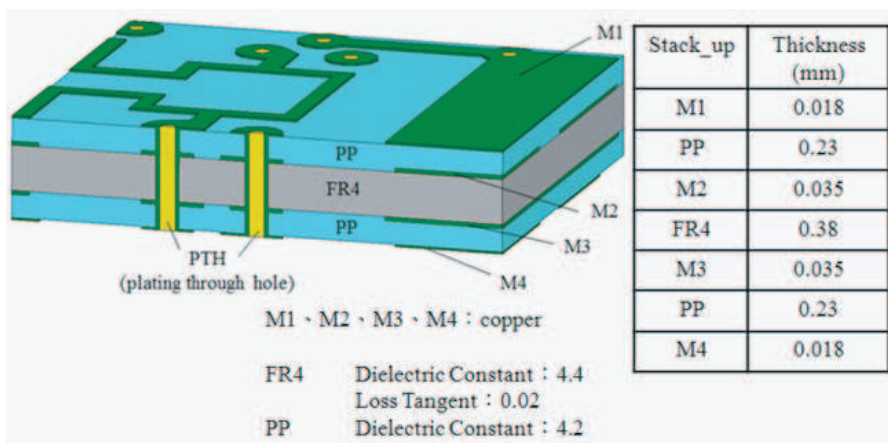


Figure 1. Cross-section of the FR4 substrate.

loss (S_{dd}^{21}) is above -10 dB and does not meet the filter specification in the high stopband. Thus, two solutions are applied to the basic structure to achieve the proposed bandpass filters. The first proposed bandpass filter integrates the ground plane, while the second one employs an extra transmission zero. Details of the process are provided in later sections of this paper. The simulation results show two full differential bandpass filters with bandwidths of 18.2% and 15%, and a common-mode rejection ratio (CMRR) > 20 dB in the passband. The most important issue is area reduction. For the proposed filters, the dimensions (including I/O pads) are $6\text{ mm} \times 6.7\text{ mm}$ for the first and $6.6\text{ mm} \times 8.3\text{ mm}$ for the second. Compared with full differential bandpass filters in other studies, the proposed filters in this paper have the smallest occupied area. Area reductions of up to 98.05% and 97.72% are achieved. Furthermore, the proposed filters designed with embedded passive device technology can provide applications for SiP.

2. RESONATOR ANALYSIS

In this paper, a full differential bandpass filter designed with double magnetically coupled resonators is fabricated. The resonators are coupled as a transformer. Four types of structure can implement coupled inductors: a parallel conductor coil [23] (also known as a Shibata type), an interactive wound coil [24] (also known as a Frlan type), a stack coupled coil [25] (also known as a Finlay type), and a concentric spiral coil. In the proposed filters, stacked coupled coils are adopted because of their high coupling efficiency, permitting a great reduction of the bandpass filter.

The structure of the proposed bandpass filter consists of two resonators that are completely the same but in opposite directions. One of the resonators is discussed as representative. First, the single resonator shown in Figure 2(a) is analyzed. This single resonator

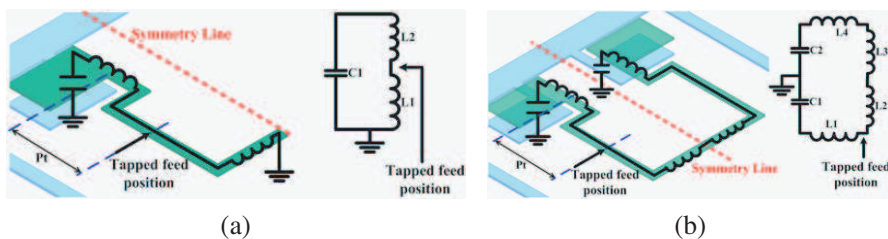


Figure 2. The structure and equivalent circuit of (a) a single resonator and (b) a double resonator.

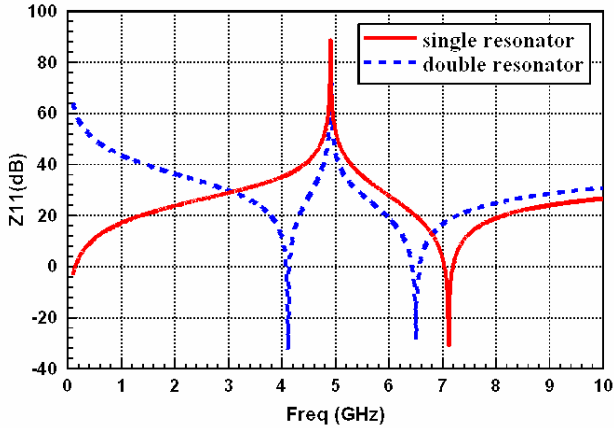


Figure 3. The input impedance of the resonator.

consists of inductors L_1 and L_2 , and a MIM capacitor C_1 ; the resonant frequency is determined by

$$f_s = \frac{1}{2\pi\sqrt{(L_1 + L_2)C}} \tag{1}$$

where f_s is the resonant frequency. The series of L_2 and C_1 provides a ratio of L_1 and L_2 . Figure 3 shows the input impedance of the single resonator and the double resonator. The double resonator is generated by mapping the single resonator along the symmetry line, as shown in Figure 2(b). Due to the symmetry property, $L_1 = L_4$, $L_2 = L_3$ and $C_1 = C_2$, the same goes for the components in the other resonator. The complete structure is derived by combining those two double resonators using a stacking method, as shown in Figure 4(a). Figure 4(b) shows the equivalent circuit of the complete circuit. The stacked structure adopted in this paper could provide proper capacitance for C_c , and shift the transmission zero in the low stopband to approach the passband. For an ideal bandpass filter, the slope at the passband edge is almost infinite. The transmission zero near the passband can make this filter ideal.

The symmetry of the physical layout is very important for a differential circuit. The proposed structure is designed on a transformer base, with the primary and secondary coils having the same number of turns. In Figure 4(b) it can be seen that the ports are put in the corresponding position at each single resonator. The signal path in each port will be the same length as in the other ports, and thus meet the requirement for a differential signal. A differential circuit

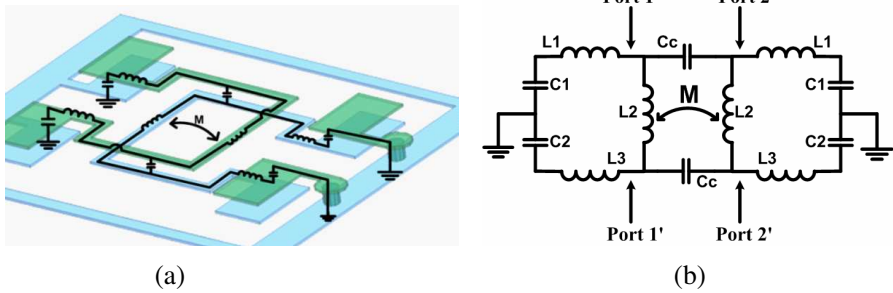


Figure 4. (a) A 3D model of the complete circuit. (b) The equivalent circuit of the full differential bandpass filter.

has two modes of operation: differential-mode and common-mode. A differential-mode acts as a signal path. On the other hand, a common-mode is regarded as noise and should be minimized. A parameter called CMRR can reveal the degree of common-mode suppression. In [26], the CMRR is defined as

$$\text{CMRR} = 20 \log \frac{|S_{21}^{dd}|}{|S_{21}^{cc}|} \quad (2)$$

S_{21}^{dd} is the insertion loss for differential-mode operation and S_{21}^{cc} is the insertion loss for common-mode operation.

3. FILTER DESIGN

In an equal-ripple Chebyshev bandpass filter prototype, the prototype element values can be derived by looking up the table with the defining order, ripple amplitude and bandwidth Δ . For example, the prototype element values are $g_0 = 1$, $g_1 = 0.843$, $g_2 = 0.622$, and $g_3 = 1.3554$ in the condition of a second-order 0.1 dB Chebyshev bandpass filter with $\Delta = 30\%$. After determining the prototype element value, the values of $Q_e = 2.81$ and $k = 0.42$ are derived using Equations (3) and (4).

$$Q_e = \frac{g_0 g_1}{\Delta} = \frac{g_2 g_3}{\Delta} \quad (3)$$

$$k = \frac{\Delta}{\sqrt{g_1 g_2}} \quad (4)$$

Q_e and k are two important parameters for a bandpass filter designed with the coupled resonator synthesis method; k is the coupling coefficient and Q_e is the external quality factor, which represents the

degree of matching with external circuits. The external quality factor Q_e is related to the tapped feed position (pt) and extracted by

$$Q_e = \frac{\omega_0 \tau \Gamma(\omega_0)}{4} (1 - y_{in}^2(\omega_0)) \tag{5}$$

where Y_{in} is the normalized input admittance, τ is the group delay, and ω_0 is the resonant angular frequency [27]. The coupling coefficient k , which decides the bandwidth of the bandpass filter, is related to the overlap area. Separating two coils can reduce the amount of coupling and thus narrow the bandwidth of the bandpass filter. The extracted value is calculated by

$$k = \pm \frac{f_{p2}^2 - f_{p1}^2}{f_{p2}^2 + f_{p1}^2} \tag{6}$$

where f_{p1} and f_{p2} are the dominant resonant frequencies [27]. Based on the above design process and fundamental structure, a full differential bandpass filter was implemented. This is the fundamental structure of the proposed bandpass filters in this paper. The detailed specifications are shown in Figure 5. While the simulation results are presented in Figure 6. Evidently, the performance in the high stopband does not fit the specification. S_{dd}^{21} in the high stopband is up to -5 dB in the simulation. Another passband is nearly formed in the high stopband. Therefore, two solutions are proposed to solve this problem.

4. TYPE I OF THE PROPOSED BANDPASS FILTER

The first solution is to integrate the ground plane completely and thus improves the ground effect. According to the design process mentioned

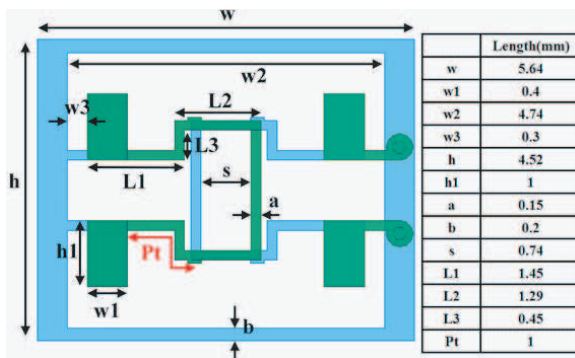


Figure 5. Layout of the basic structure.

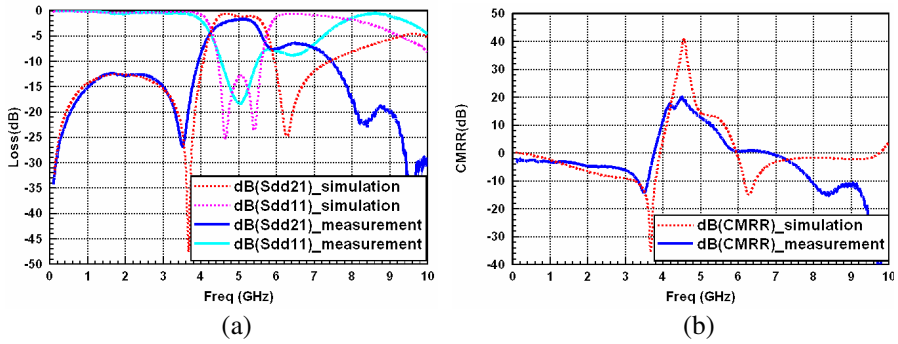


Figure 6. Results of (a) differential-mode and (b) CMRR for the original design.

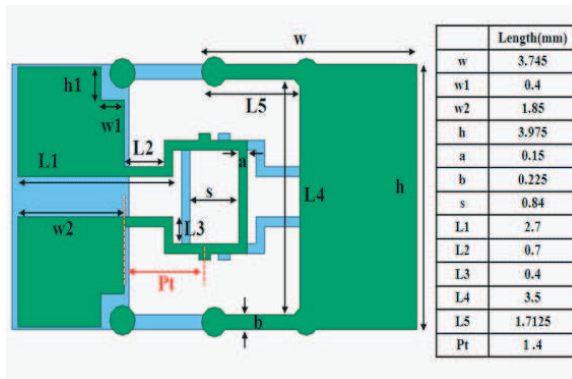


Figure 7. Layout of type I.

above, the prototype element values with bandwidth $\Delta = 20\%$ are $g_0 = 1$, $g_1 = 0.843$, $g_2 = 0.622$ and $g_3 = 1.3554$. $Q_e = 4.2$ and $k = 0.28$ are calculated based on Equation (3) and (4). In this design, the tapped feed position is placed 1.4 mm away from the capacitor, and the overlap area of two coils is about 1.94 mm^2 . According to Equations (5) and (6), the extracted value of Q_e and k are respectively 4.47 and 0.21, which conform to the theory. The detailed specifications of the full differential bandpass filter after its redesign are shown in Figure 7. This bandpass filter was fabricated on FR4 with four layers of metal. The main coils were put on the second and third layers to prevent them being affected by the PP glue. Because of the stacked structure, the occupied area of the bandpass filter is only about $6.7 \text{ mm} \times 7 \text{ mm}$. However, the arrangement of the integrated ground plane decreases the symmetry slightly. As shown in Figure 7, the right side of the

second-layer circuit is the integrated ground plane while the left side is the upper plate of the capacitors, which is designed in two pieces. The difference between the right side and the left side causes an imbalance and reduces the ability for common-mode suppression. Consequently, the maximum CMRR value is lower than in the original design, but the CMRR of this design maintains 20 dB in the passband, as shown in Figure 8(b). The differential-mode result is shown in Figure 8(a). The passband is in the range of 4.39 GHz to 5.3 GHz, with two transmission zeros at 3.66 GHz and 5.81 GHz.

5. TYPE II OF THE PROPOSED BANDPASS FILTER

The other solution is to employ an extra transmission zero to suppress S_{dd}^{21} in the high stopband. The extra transmission zero is formed by connecting an inductor and a capacitor. The parallel LC is connected from one tapped feed position to the ground and utilized on the first layer. The position of the extra transmission zero in the frequency response can easily be shifted by changing the length of the inductor or the area of the capacitor. Figure 9 demonstrates the situation of shifting the position of the extra transmission zero by changing the capacitor area. Locating an appropriate position for the extra transmission zero will enhance the performance of the bandpass filter.

According to the design process mentioned in the previous section, the prototype element values with fractional bandwidth $\Delta = 18\%$ are $g_0 = 1$, $g_1 = 0.843$, $g_2 = 0.622$, and $g_3 = 1.3554$. $Q_e = 4.68$ and $k = 0.249$, calculated using Equations (3) and (4). The Q_e and k are the same as previously indicated. The appropriate values of those two parameters in this design are $Q_e = 3.92$ and $k = 0.245$, with the tapped feed position 1.75 mm and the overlap area 1.58 mm^2 . The detailed

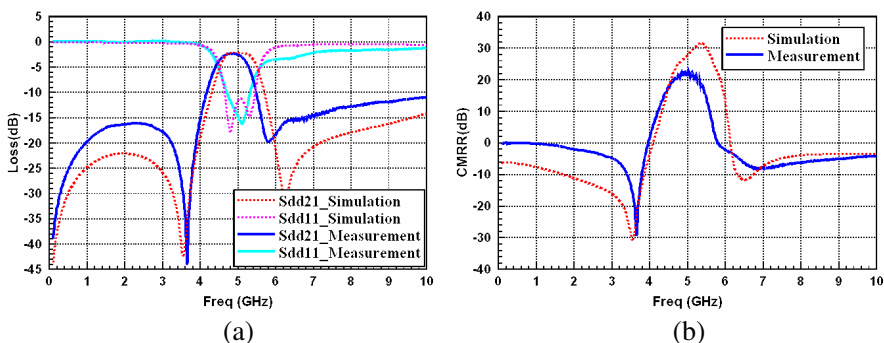


Figure 8. Results for (a) differential-mode and (b) CMRR in type I.

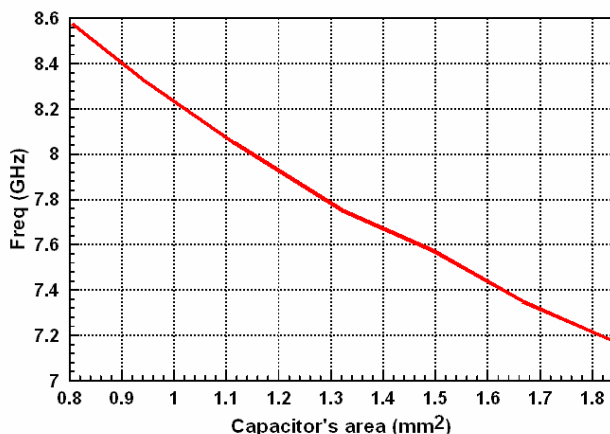


Figure 9. Shifting the extra transmission zero by changing the capacitor area.

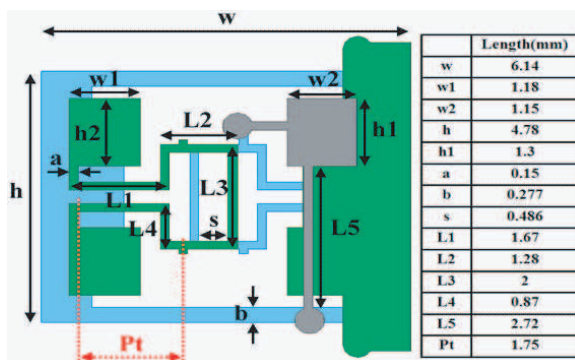


Figure 10. Layout of type II.

specifications for this filter are shown in Figure 10, and the simulation and measurement results are given in Figure 11. The simulation results show a bandwidth of 15% from 4.88 GHz to 5.56 GHz and a CMRR above 20 dB. To optimize performance, the extra transmission zero is designed at 7.8 GHz while the two original transmission zeros are at 4.3 GHz and 6.2 GHz. In the measurement results, the extra transmission zero is shifted to 8 GHz and the CMRR is about 20 dB in the passband. Overall, the tendencies of the measured and simulation results are similar.

After all of the designs and layouts were decided, the I/O ports were laid on the fourth layer. This arrangement made for convenient

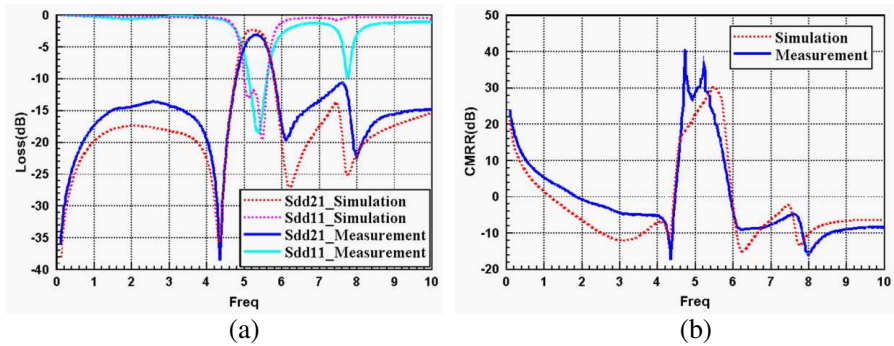


Figure 11. Results of (a) differential-mode and (b) CMRR.

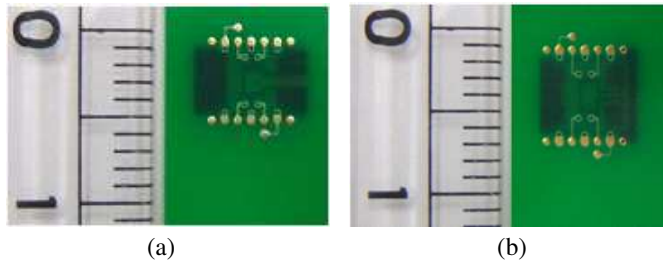


Figure 12. Photographs of (a) type I and (b) type II, with scale provided.

measurement or integration with other circuits. The I/O pads were designed in the shape shown in Figure 12. The circles were pads of solder bumps, prepared for integration with other circuits for SiP applications.

6. DISCUSSION

Two full differential bandpass filters were fabricated, having CMRRs above 20 dB and passbands that fit with the WLAN IEEE 802.11a (5 GHz) standard. As Figure 12 shows, the dimensions of the proposed bandpass filters were 6 mm × 6.7 mm and 6.6 mm × 8.3 mm. Table 1 provides the comparisons of the results for the full differential bandpass filters in this paper and in previous studies. Clearly, the bandpass filters in this paper occupy the smallest area. The proposed bandpass filters were both implemented on FR4. Compared with the circuits implemented on RT/duroid 6010, the type I proposed filter had area reduction of 61.3%, 78.9%, and 91.7%, and the type II had area reductions of 47.3%, 71.24%, and 88.86%. For the designs also

Table 1. Comparisons of type I and type II with other references.

	f_0 (GHz)	BW (%)	Substrate	Structure
Type I	5	18.2	FR4	double coupled resonators
Type II	5.2	15	FR4	double coupled resonators
[5]	5.4	24.4	RT/duroid 6010	CPWstepped Impedance resonators
[15]	4	65	RT/duroid 6010	microstrip line
[14]	4.1	61.7	RT/duroid 6010	microstrip line
[28]	4.5	53	FR-4	U-shaped and H-shaped patterned ground structure
	Dimension (mm ²)	$\frac{\text{Type I}}{\text{other design}}$ (%)	CMRR	-
Type I	6 × 6.7 (40.2)	reference	20 dB	-
Type II	6.6 × 8.3 ((54.78))		20 dB	-
[5]	9.9 × 10.5 (103.95)	38.7%	20 dB	-
[15]	13.8 × 13.8 (190.44)	21.1%	N/A	-
[14]	20 × 24 (480)	8.3%	20 dB	-
[28]	40 × 60 (2400)	1.68%	20 dB	-

implemented on FR4, the area reductions of the two proposed filters were as high as 98.32% and 97.72% respectively. The RT/duroid 6010 substrate has a higher dielectric constant than FR4, but RT/duroid 6010 costs more than FR4. This paper concludes that the proposed full differential bandpass filters can achieve significant area reduction and can be fabricated at low cost.

7. CONCLUSION

In this paper, a very compact, full differential bandpass filters structure was designed, and two methods were adopted to solve the problem of poor high-frequency response. The first method was to integrate the ground plane to enhance the effect of grounding. The second method was to employ an extra parallel LC resonator to create an extra transmission zero and then suppress the high-frequency response. Both of these two proposed full differential bandpass filters were fabricated on FR4. Area reduction was attributable to the use of a stacked structure. As Table 1 illustrated, the occupied areas of the bandpass filters were $6.7 \text{ mm} \times 7 \text{ mm}$ and $6.6 \text{ mm} \times 8.3 \text{ mm}$, providing a maximum area reduction of 98.05% and 97.76%. In the terms of application, the passbands in the 4.88–5.65 GHz and 4.3–5.3 GHz ranges both conform to the WLAN IEEE 802.11a (5 GHz) protocol. Finally, the I/O ports of the bandpass filters in this paper were purposely designed for circuit integration in SiP application.

REFERENCES

1. Shairi, N. A., et al., "RF receiver system design for wireless local area network bridge at 5725 to 5825 MHz," *Asia-Pacific Conference on Applied Electromagnetics 2007, APACE 2007*, 1–6, 2007.
2. Razavi, B., *Design of Analog CMOS Integrated Circuits*, McGraw-Hill Higher Education, 2003.
3. Sedra, A. S. and K. C. Smith, *Microelectronic Circuits*, Oxford University Press, 1998.
4. Gilbert, B., "A precise four-quadrant multiplier with subnanosecond response," *IEEE Journal of Solid-State Circuits*, Vol. 3, 365–373, 1968.
5. Chen, C.-J., S.-W. Wang, C.-H. Lee, C.-I. G. Hsu, H.-H. Chen, "Wideband balanced BPF design for MB-OFDM applications," *Asia-Pacific Microwave Conference Proceedings (APMC)*, 1082–1085, 2010.

6. Chiou, Y.-C., P.-S. Yang, J.-T. Kuo, and C.-Y. Wu, "Transmission zero design graph for dual-mode dual-band filter with periodic stepped-impedance ring resonator," *Progress In Electromagnetics Research*, Vol. 108, 23–36, 2010.
7. Velazquez-Ahumada, M. D. C., J. Martel-Villagr, F. Medina, and F. Mesa, "Design of band-pass filters using stepped impedance resonators with floating conductors," *Progress In Electromagnetics Research*, Vol. 105, 31–48, 2010.
8. Velazquez-Ahumada, M. D. C., J. Martel-Villagr, F. Medina, and F. Mesa, "Application of stub loaded folded stepped impedance resonators to dual band filters," *Progress In Electromagnetics Research*, Vol. 102, 107–124, 2010.
9. Kung, C.-Y., Y.-C. Chen, S.-M. Wu, C.-F. Yang, and J.-S. Sun, "A novel compact 2.4/5.2 GHz dual wideband bandpass filter with deep transmission zero," *Journal of Electromagnetic Waves and Applications*, Vol. 25, No. 5–6, 617–628, 2011.
10. Lee, C.-H., C.-I. G. Hsu, H.-H. Chen, and Y.-S. Lin, "Balanced single- and dual-band BPFs using ring resonators," *Progress In Electromagnetics Research*, Vol. 116, 333–346, 2011.
11. Yang, C.-F., Y.-C. Chen, C.-Y. Kung, J.-J. Lin, and T.-P. Sun, "Design and fabrication of a compact quad-band bandpass filter using two different parallel positioned resonators," *Progress In Electromagnetics Research*, Vol. 115, 159–172, 2011.
12. Peik, S. F. and F. A. Langner, "New differential PSL coupled resonator filters," *IEEE MTT-S International Microwave Symposium Digest*, 447–450, 2008.
13. Shi, J., et al., "A novel differential bandpass filter based on double-sided parallel-strip line dual-mode resonator," *Microwave and Optical Technology Letters*, Vol. 50, 1733–1735, 2008.
14. Lim, T. B. and L. Zhu, "Highly selective differential-mode wideband bandpass filter for UWB application," *IEEE Microwave and Wireless Components Letters*, Vol. 21, 133–135.
15. Lim, T. B. and L. Zhu, "A differential-mode wideband bandpass filter on microstrip line for UWB application," *IEEE Microwave and Wireless Components Letters*, Vol. 19, 632–634, 2009.
16. Lim, T. B. and L. Zhu, "Differential-mode ultra-wideband bandpass filter on microstrip line," *Electronics Letters*, Vol. 45, 1124–1125, 2009.
17. Lim, T. B. and L. Zhu, "Differential-mode wideband bandpass filter with three transmission zeros under common-mode operation," *Asia-Pacific Microwave Conference Proceedings (APMC)*,

- 159–162, 2009.
18. Lopez-Berrocal, B., J. de-Oliva-Rubio, E. Marquez-Segura, A. Moscoso-Martir, I. Molina-Fernandez, and P. Uhlig, “High performance 1.8–18 GHz 10-dB low temperature co-fired ceramic directional coupler,” *Progress In Electromagnetics Research*, Vol. 104, 99–112, 2010.
 19. Wang, Z., P. Li, R.-M. Xu, and W. Lin, “A compact X-band receiver front-end module based on low temperature co-fired ceramic technology,” *Progress In Electromagnetics Research*, Vol. 92, 167–180, 2009.
 20. Rosser, S. G., et al., “Miniaturization of printed wiring board assemblies into system in a package (sip),” *European Microelectronics and Packaging Conference 2009, EMPC 2009*, 1–8, 2009.
 21. Sham, M. X., et al., “Challenges and opportunities in System-in-Package (SiP) business,” *7th International Conference on Electronic Packaging Technology 2006, ICEPT’06*, 1–5, 2006.
 22. Wu, S.-M., C.-T. Kuo, and C.-H. Chen, “Very compact full differential bandpass filter with transformer integrated using integrated passive device technology,” *Progress In Electromagnetics Research*, Vol. 113, 251–267, 2011.
 23. Shibata, K., et al., “Microstrip spiral directional coupler,” *IEEE Transactions on Microwave Theory and Techniques*, Vol. 29, 680–689, 1981.
 24. Frlan, E., et al., “Computer aided design of square spiral transformers and inductors [MIC application],” *IEEE MTT-S International Microwave Symposium Digest*, Vol. 2, 661–664, 1989.
 25. Geen, M. W., et al., “Miniature multilayer spiral inductors for GaAs MMICs,” *11th Annual Technical Digest 1989 Gallium Arsenide Integrated Circuit (GaAs IC) Symposium*, 303–306, 1989.
 26. Eisenstadt, W. R., et al., *Microwave Differential Circuit Design Using Mixed-mode S-parameter*, Artech House Publishers, 2006.
 27. Hong, J.-S. G. and M. J. Lancaster, *Microstrip Filters for RF/Microwave Applications*, Wiley-Interscience, 2001.
 28. Wu, S.-J., et al., “A novel wideband common-mode suppression filter for gigahertz differential signals using coupled patterned ground structure,” *IEEE Transactions on Microwave Theory and Techniques*, Vol. 57, 848–855, 2009.